Arabian Journal of Geosciences (2018) 11: 25
https://doi.org/10.1007/s12517-017-3378-1

ORIGINAL PAPER

Petrology of calc-alkaline/adakitic basement hosting A-type Neoproterozoic granites of the Malani igneous suite in Nagar Parkar, SE Sindh, Pakistan

M. Qasim Jan[1] · Amanullah Laghari[2] · M. Asif Khan[3] · M. Hassan Agheem[2] · Tahseenullah Khan[4]

Received: 9 February 2017 / Accepted: 28 December 2017 / Published online: 11 January 2018

Abstract
The Nagar Parkar area contains three distinct groups of rocks, from oldest to youngest, (1) basement rocks ranging in composition from mafic to (quartz)diorite, tonalite, granite, and younger granodiorite, (2) granite plutons similar in general features to those of the Malani Igneous Suite of Rajasthan, and (3) abundant mafic, felsic and rhyolitic dykes. The basement rocks show strong brittle and local plastic deformation, and epidote amphibolite/upper greenschist facies metamorphic overprint. The chemistry of the basement rocks contrasts the commonly agreed within plate A-type character of the Neoproterozoic granites (group 2) that are emplaced into them. The basement rock association is calc-alkaline; the granodiorite displays the compositional characteristics of adakites, whereas the tonalite has intermediate composition between typical adakite and classical island arc rocks. This paper presents detailed petrography of the basement rocks and compares their geochemistry with those of the group 2 granites as well as with rocks from other tectonic environments. It is proposed that the Nagar Parkar basement is part of a 900–840 Ma magmatic arc that was deformed before it was intruded 800–700 Ma ago by the A-type continental granitic rocks followed by mafic to felsic dykes.

Keywords Nagar Parkar · Pakistan · Arc-related basement · Petrology · Malani igneous suite

Introduction

Nagar Parkar area covers 500 km^2 of the border zone of the Great Rann of Kutch and Thar Desert in SE Sindh, Pakistan. The landscape is characterized by the presence of mounds and bold hills abutting a flat plain covered by sand, silt and salt. The area contains mafic to silicic rocks that constitute basement for Neoproterozoic granite intrusions and younger mafic and felsic dykes (Fig. 1). The rocks have been collectively referred to as Nagar Parkar igneous complex–NPIC (cf., Kazmi and Jan 1997). The geology and mineral deposits of the area have been studied by several workers (Kazmi and Khan 1973; Jan et al. 1997; Ahmad and Chaudhry 2008; Khan et al. 2012), and the granites have been regarded as the southwestern extension of the Malani Igneous Suite (MIS) of the adjacent Rajasthan (Butt et al. 1994; Laghari 2004; Kochhar 2009; Jan et al. 2016, 2017).

The basement rocks are mostly exposed in the flat ground from which sand cover has been removed by erosion (Fig. 2a, b), but they locally also occur in the mounds. They comprise mostly amphibolite and hornblende diorite (Fig. 2c), with many small granitoid intrusions, and local outcrops of metasedimentary rocks in the Dhedvero area. Medium- to fine-grained mafic to intermediate rocks of the basement also occur as blocks and cm-size xenoliths enclosed in granites (Jan et al. 2014). The Nagar Parkar granites occur as dykes, bosses and stocks that form subdued to bold hills, of which the Karunjhar hill attains a height of 262 m above sea level. They are represented by several varieties, the more abundant being

✉ M. Qasim Jan
mqjan@yahoo.com

[1] National Centre of Excellence in Geology, University of Peshawar, Peshawar, & COMSTECH, Islamabad, Pakistan

[2] Centre for Pure and Applied Geology, University of Sindh, Jamshoro, Pakistan

[3] National Centre of Excellence in Geology, University of Peshawar, Peshawar, Pakistan

[4] Department of Earth and Environmental Sciences, Bahria University, Islamabad, Pakistan

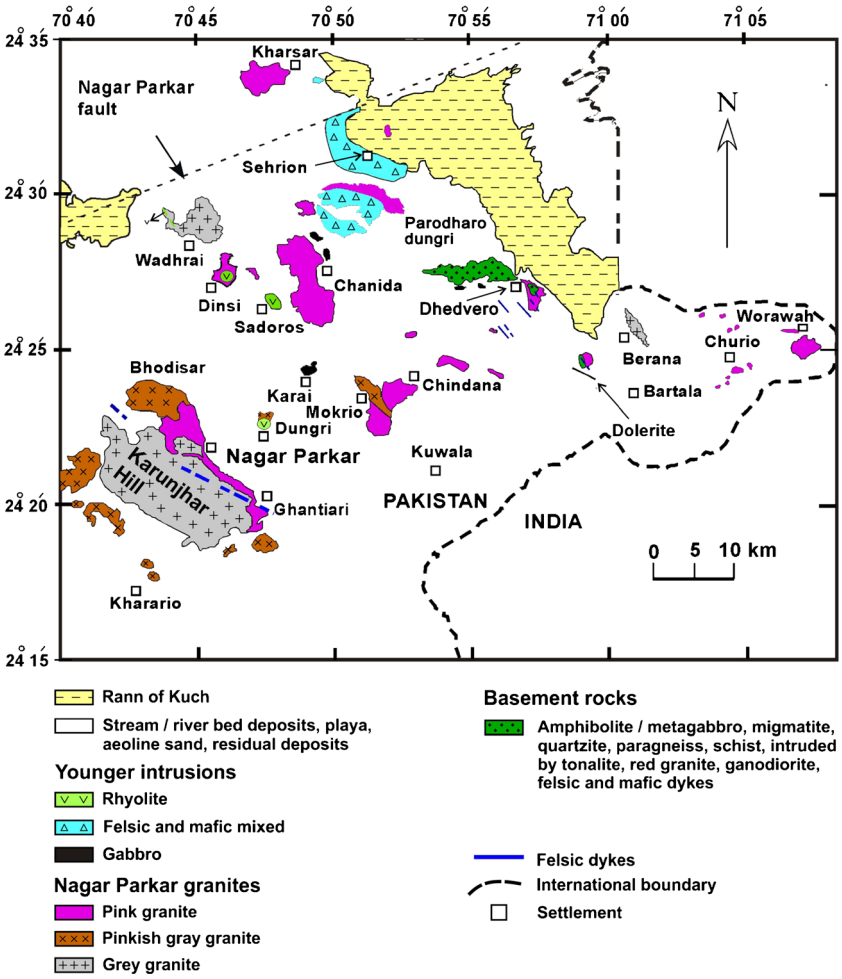

Fig. 1 Simplified geological map of the Nagar Parkar Igneous Complex (modified after Khan et al. 2012)

gray riebeckite-aegirine granite, pinkish gray biotite-hornblende granite/quartz monzonite, and pink biotite ± hornblende granite. Many felsic (microgranite, aplite, rare pegmatite), mafic and rhyolitic dykes are emplaced into the granites and the basement. On the basis of similarity in petrography and color, the gray granites were equated with those of Erinpura and the pink with Jalor pluton in Rajasthan (Laghari 2004).

In the past, not much attention was paid to the petrology of the basement rocks hosting the Neoproterozoic granite intrusions. However, while the latter are undeformed, commonly alkaline and have been regarded as A-type (Laghari 2004; Ahmad and Chaudhry 2008; Khan et al. 2012), the present study shows that in addition to greater variation in rock-types, the basement has undergone plastic and brittle deformation (Figs. 2d–h and 3a–d) prior to the emplacement of the granites. We combine petrographic and geochemical data on the basement rocks for gaining new insight into the NPIC, and show that the basement (meta) igneous rocks are calc-alkaline and geochemically different from the two major varieties of the Neoproterozoic gray and pink granites which intrude them. The trace and rare earth element geochemistry of the rocks is compared with granitic rocks from within plate and arc tectonic environments.

Field features

The basement rocks appear to occupy much of the level ground since they crop out in patches and, locally, in mounds all over the Nagar Parkar area. They are particularly well exposed and abundant in a 10 km^2 area around Dhedvero village (24° 26′ 57″ N, 70° 46′ 33″ E). Some basement rocks occur in narrow strips in the plain area (e.g., north of Dhedvero) and in patches mixed with granite intrusions in the centrally located flat zones. The basement mostly comprises hornblende gabbro to dioritic/amphibolitic rocks and intrusive bodies of tonalite, patches and dykes of red granite, and hornblende-biotite granodiorite (Fig. 2a, b). There are a few small (meters-size) pools of hornblendite. These rocks are associated locally with migmatites, paragneiss, schist and quartzites in the Dhedvero area. The igneous rocks in the basement are medium- to fine-

Fig. 2 Photographs, mostly from Dhedvero area, showing field features of the basement hosting Neoproterozoic granites. **a** Amphibolitic basement rocks (some in blocks) in the foreground and Nagar Parkar plain and Runpur granite body in the background. **b** General view of the basement, dominantly comprising here amphibolitic-dioritic rocks that have gentle topography due to erosion and weathering. **c** Fractured, but otherwise undeformed metagabbro cut by dolerite dyke (center). **d** Tonalite/quartz diorite block showing shear banding and felsic veins. Note that a felsic vein near the pen seems folded on the left side. **e** Felsic dykelet in amphibolitic rock showing folding. **f** Plastic deformation and shear banding in a tonalite dyke in mafic rocks, west of Dhedvero. Coin is for scale. **g**, **h** Migmatitic basement east of Dhedvero, showing two phases of plastic deformation. The leucosomes at places are showing tight isoclinal folding (F1) that has later been gently folded (F2)

grained, with veins and small patches of coarser material. They also contain cm-thick veins comprising one or more of the minerals epidote, quartz, and chlorite. Sheets (up to 2 km × 6 m) of brown-red rhyolite-quartz trachyte, extending in N12°W direction, cut the Dhedvero basement and appear to be younger like the microgranite and dolerite dykes so common in the NPIC.

The field and petrographic aspect of the basement rocks are shown in Figs. 2 and 3. Most rocks are jointed, highly fractured, sheared, and at places banded and foliated. In addition to brittle deformation (Figs. 2d and 3a–d, the rocks locally also show plastic deformation and, sparingly, are migmatized (Fig. 2d–h). They contain two distinct cleavages within the local 'gneissose' fabric which itself is sparingly folded tightly (Butt et al. 1989). Some of the rocks display at least two phases of plastic deformation (Fig. 2g–h). The red granite dykes of the basement (Fig. 3a) are characterized by brittle deformation, local planer fabric (and low-grade metamorphic overprint) like the rest of the basement. Fracturing and brittle deformation have rendered the basement rocks readily susceptible to erosion, hence their common occurrence in the peneplained areas. On petrologic grounds, the 2 × 1 km granodiorite boss near Parodharo is also here considered as part of the basement despite its fresh and undeformed nature. Since the deformed basement locally contains small bodies of rocks that look similar to it, this body may have survived shear deformation as a mega-boudin or it may have been emplaced after deformation. It has been reported (Ashwal et al. 2013) that the Mt. Abu granitoid in Rajasthan consists of deformed and undeformed varieties. Further information on the field features of the basement can be seen in Muslim et al. (1997) and Laghari (2004).

Petrography

The basement rocks are medium- to fine-grained, inequigranular to subequigranular, and hypidiomorphic to allotriomorphic in texture. Shearing has obliterated original textures in many, but some rocks appear to have been porphyritic. The mafic and dioritic members are composed mainly of plagioclase and amphibole, with small amounts of quartz,

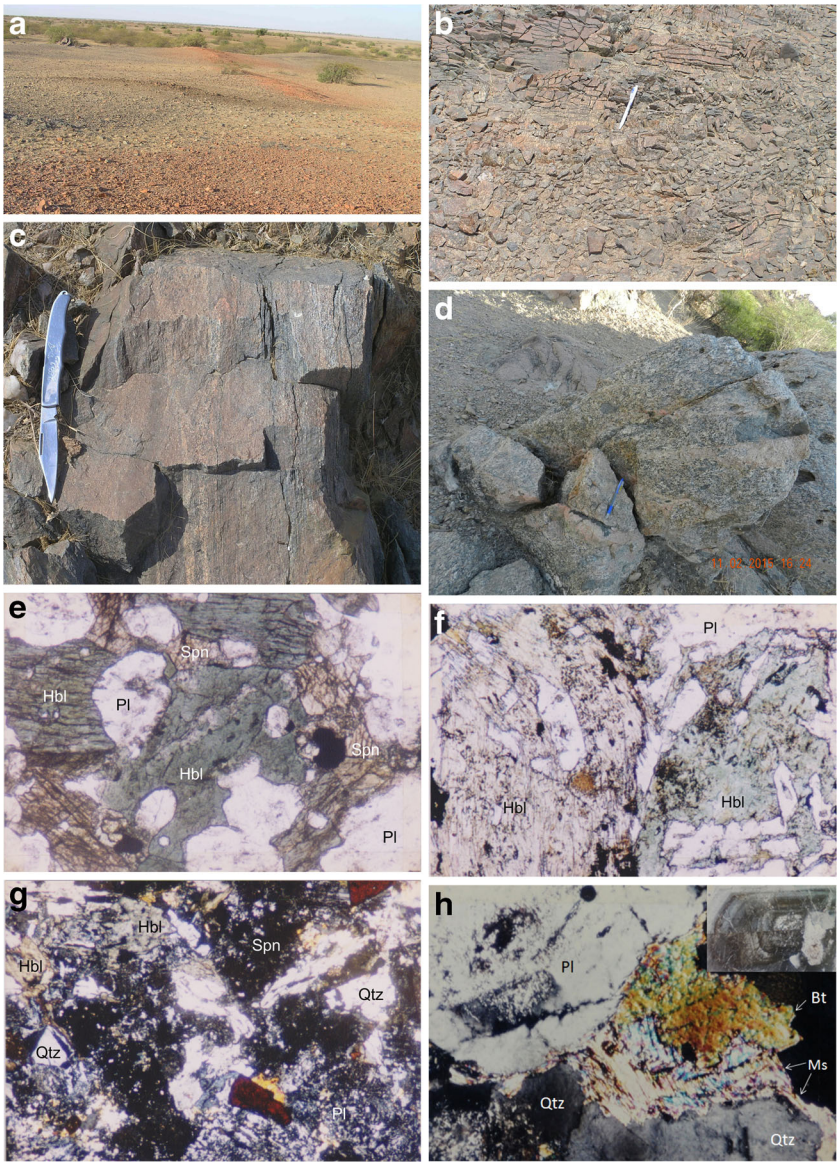

Fig. 3 Field photos and photomicrographs of the basement. **a** Highly jointed and flattened basement comprising a mixture of mafic (dark gray) rocks and abundant intrusions of the red granite near Jodhe-jo-Wandhio. **B**: **b** Mafic rocks of Fig. 3a showing pervasive fracturing and jointing resulting from brittle deformation. **c** Quartz diorite/tonalite basement dyke in amphibolitic rocks near Dhedvero, showing shear banding and foliation. **d** Quartz diorite showing shear foliation, mafic xenoliths and granitic dykes. This picture is from a hundreds of meters large roof pendent(?) of the basement in the northern part of the Ranpur pluton. **e** Mafic rock from Dhedvero containing slightly altered hornblende (Hbl, green) and plagioclase (Pl, white, partly cloudy), titanite (Spn, yellow brown) and iron oxide. Note inclusions of quartz and iron oxide in hornblende. The plagioclase is mostly untwined and cloudy, but a few grains (top left) have clear (albitic?) margins. Plane light. Length of the picture is 1.25 mm. **f** Slightly altered dioritic rock containing hornblende (Hbl, yellow and green), opaque oxides, and plagioclase (Pl). The hornblende grain on the left shows bending in the upper part. Plane light. Field of view is 2.25 mm long. **g** Altered rock from Dhedvero basement. Yellowish green hornblende (Hbl, top left) is a little altered to chlorite. Plagioclase (Pl) is completely altered to epidote and sericite. Dark areas are opaque oxides altered to titanite (Spn). Quartz is fresh. Reddish, euhedral Fe-Ti-oxide in lower centre and top right. Plane light. Field of view is 2.25 mm. **h** Parodharo granodiorite containing zoned, medium-plagioclase with altered cores, quartz, biotite, muscovite, hornblende (not visible) and opaque oxide (rounded grain in top centre). Crossed polars, field of view 2.25 mm. Inset is a 1.25-mm long plagioclase crystal showing oscillatory zoning and Carlsbad twinning

epidote, augititic clinopyroxene, chlorite, biotite, titanite, and iron oxide (Fig. 3e–g). The clinopyroxene is consumed by hornblende, similar to hornblende sponges described by from island arcs (Smith 2014; Davidson et al. 2007). Rutile, leucoxene, zircon, and apatite are minor accessories, along with allanite and secondary carbonate in some rocks. Epidote and chlorite are locally abundant. Some samples have thin veins of quartz and/or epidote, with or without minor

amounts of other minerals. Quartz is abundant in the granitoid members (tonalite, granodiorite, granite) and accompanied by sericitized K-feldspar. The hornblendites are essentially composed of amphibole with minor opaque oxide and, in some, clinopyroxene.

The rocks show overprinting of secondary minerals developed probably during metamorphism or uplift. It appears that much of the brittle shearing and jointing occurred after the plastic deformation and metamorphic overprinting. Plagioclase and hornblende are locally deformed and strained, and show bending and fracturing in elongated grains. The plagioclase is generally cloudy due to epidotization and saussuritization, but fresh plagioclase with weakly developed zoning is also present. Small grains of the amphibole are generally fresh, but the larger ones are altered locally to epidote and chlorite, and may be uralitized at the margins. The amphibole is, thus, of two generations and shows evidence of growth prior to, as well as along with, epidote. The primary amphibole (hornblende) is pleochroic from green to dark or yellowish green, whereas the second generation amphibole (actinolite?) is light green to green. Epidote, occurring as subhedral grains, contains small inclusions of cloudy plagioclase, titanite and amphibole. Another generation of epidote and sericite developed due to alteration of plagioclase. Anhedral flakes of chlorite are generally associated with the amphibole and sparingly with epidote. Titanite, both primary and secondary, is a common accessory mineral in all the rocks. Rutile, magnetite and ilmenite occur in variable amounts; some as small secondary grains in the amphibole along fractures, cleavages and grain boundaries, but independent grains of the latter two accessory phases are also common (Fig. 3e).

The development of epidote and actinolitic amphibole at the expense of plagioclase, hornblende and clinopyroxene, the common association of epidote and second generation amphibole, and the presence of some fresh (sodic?) plagioclase indicate that the rocks underwent epidote amphibolite facies or high greenschist facies metamorphism. Some chlorite, saussurite, sericite and leucoxene may have formed during the uplift of the rocks. The Parodharo pluton is composed of rather uniform hornblende-biotite granodiorite showing no obvious deformation, however, the grains in thin section show non-uniform extinction (Fig. 3h). The plagioclase shows oscillatory zoning and is commonly altered in the cores.

Geochemistry of the basement

Representative rock specimens were geochemically analyzed (Table 1). Samples 1 to 10 were collected from the deformed basement, whereas samples 11 to 14 are from the undeformed Parodharo body in the basement.

Analytical techniques

Powder pellets of samples 1–5 and 10 were analyzed by WD-XRF, controlled by software Spectra^{Plus}, and setting the minimum and maximum voltage and current as 15–60 Kv and 20–150 mA, respectively. The rest of the samples were wet chemically analyzed, using atomic absorption, but alkalis were measured by flame photometry and SiO_2 was determined gravimetrically. Two of the samples (8 and 11) were also analyzed for trace and rare-earth elements by inductively coupled plasma. In all cases, routine procedures were followed, and international standards were used for control. Total iron, determined as Fe_2O_3 in the XRF analyses, was split into FeO and Fe_2O_3 for CIPW norms calculation (Irvine and Barager 1971).

Major elements geochemistry

The analyzed rocks range from basic to silicic in composition. All the analyses contain hypersthene, magnetite and ilmenite in the norms. The basement analyses, except No. 10 (red granite), contain diopside. The six mafic rock analyses contain 2.7 to 5.3 wt% $Na_2O + K_2O$, however, none is nepheline normative. Analysis 4 contains 1.8% of normative quartz, whereas the other five contain 0.1 to 14.1% normative olivine. The remaining eight analyses are silicic in composition and characterized by 25.6 to 41.8% of normative quarts. The Parodharo granodiorite contains 0.4 to 2.3% normative corundum and the red granite 1.95% of it. A distinct difference in the analyses of the tonalite and the granodiorite is that the former are diopside normative whereas the latter are corundum normative. The MgO contents and Mg# of the granodiorite analyses are lower and K_2O/Na_2O ratios higher than those of the tonalite. In the following, we shall point out some similarities between the basement granitoids and adakitic rocks (Martin 1999).

Plots of the analyses on the classification scheme involving expression of the whole-rock chemical composition into cationic proportions are shown in Fig. 4. The regrouping of the cations (De la Roche et al. 1980) is such that X-axis [R1 = 4Si – 11(Na + K) – 2(Fe + Ti)] of the diagram reflects variation in quartz content, while the Y-axis [R2 = 6Ca + 2(Mg + Al)] displays variation in Mg/Fe ratio and An content of the constituent plagioclase. In this scheme, the Parodharo samples classify as granodiorite, the mafic rocks classify as olivine gabbro and gabbro-diorite, whereas three of the basement granitoids classify as tonalite and one as granite. Five of the mafic rock analyses fall below the Ab-An line, whereas one shows mildly alkaline character. Plots of the analyses on Debon and Le Fort (1988) classification yield similar results.

The SiO_2 – A.R. [A.R. = $(Al_2O_3 + CaO + Na_2O + K_2O)/(Al_2O_3 + CaO + Na_2O - K_2O)$] diagram was devised

Table 1 Analyses and CIPW norms of selected samples from Nagar Parkar basement

Oxide %	1	2	3	4	5	6	7	8	9	10	11	12	13	14
SiO_2	44.26	48.95	49.23	49.96	50.87	50.78	65.50	65.90	67.52	77.87	73.12	71.32	70.89	70.02
TiO_2	2.59	1.67	1.54	1.45	1.75	1.12	0.29	0.31	0.83	0.17	0.32	0.41	0.42	0.47
Al_2O_3	14.31	15.24	15.48	15.79	15.39	17.12	15.02	13.30	14.82	12.77	14.32	15.89	15.78	15.28
Fe_2O_3	18.50	10.29	11.50	14.18	10.16	6.48	5.25	5.44	3.81	0.77	1.41	2.04	2.30	2.43
MnO	0.28	0.23	0.22	0.19	0.24	0.12	0.10	0.09	0.08	0.01	0.05	0.07	0.09	0.07
MgO	6.05	10.00	8.89	4.78	9.70	8.38	3.39	3.64	1.78	0.14	0.66	0.65	0.79	0.79
CaO	10.30	6.98	6.28	9.27	7.39	7.69	5.51	6.00	4.63	0.58	2.48	2.28	2.61	2.62
Na_2O	2.03	2.24	2.47	2.67	2.46	3.45	3.34	3.41	3.98	3.20	4.65	4.36	4.46	4.78
K_2O	0.67	0.99	1.99	0.65	1.16	1.87	0.52	0.43	1.26	4.17	1.82	2.23	2.03	1.91
P_2O_5	0.10	0.62	0.59	0.19	0.56	0.18	0.24	0.07	0.30	0.01	0.08	0.06	0.33	0.19
LOI	0.93	2.79	1.81	0.88	0.32	2.37	0.85	0.89	0.81	0.30	0.92	0.77	0.74	0.82
Total	100.02	100.00	100.00	100.01	100.00	99.56	100.01	99.48	99.82	99.99	99.83	100.08	100.44	99.38
C.I.P.W. norms														
Q				1.78			25.62	25.94	27.11	41.75	32.88	31.15	30.40	28.05
Or	4.06	6.08	12.11	3.93	6.94	11.44	3.12	2.59	7.55	24.76	10.90	13.30	12.07	11.49
Ab	17.59	19.65	21.47	23.04	21.03	30.17	28.60	29.37	34.08	27.15	39.78	37.17	37.88	41.07
An	28.62	29.64	25.95	29.75	27.81	26.55	24.74	20.06	19.07	2.83	11.99	11.06	11.07	12.09
C										1.95	0.35	2.29	2.21	1.00
Di	19.32	2.04	2.06	13.41	4.81	9.47	1.07	8.07	2.00					
Hy	6.67	34.28	23.15	21.37	32.07	7.38	14.36	11.94	6.92	1.01	2.93	3.57	4.25	4.33
Ol	13.77	0.93	8.01		0.12	14.06								
Mt	4.70	2.70	2.92	3.47	2.64	1.71	1.22	1.27	1.02	0.21	0.38	0.54	0.59	0.64
Il	5.02	3.29	3.01	2.81	3.36	2.20	0.56	0.60	1.60	0.32	0.62	0.79	0.80	0.91
Ap	0.22	1.40	1.32	0.42	1.24	0.41	0.53	0.16	0.66	0.02	0.18	0.13	0.72	0.42
Trace elements (in ppm)														
Nb	6			5				1.9		5.5	3.2			
Zr	64			75				20		113.1	20			
Y	18			19				13		30.9	6.8			
Sr	412			447				307		100.3	295			
Rb	11			10				8.2		45.9	15.5			
Zn	124			102						10.8				
Ba	113			393				120		2418	729			
Cu	38			53						4.2				
Co	48			45						272.4				
Ce	8			30				17.1		66.6	25.2			
Th	2			3				0.4		8.2	2.5			
Nd	20			11				12.9		32.1	14.9			
Ga	20			20						11.2				
U	1			2						2.1				

No. 8 also contains (in ppm) Cr 54, Ni 21, Ta 1.8, Hf 0.7, La 9.2, Ce 17.1, Pr 2.5, Sm 2.7, Eu 0.7, Tb 0.4, Gd 2.5, Dy 2.1, Ho 0.5, Er 1.3, Yb 1.3

No. 11 also contains (in ppm) Cr 6, Ni, < 5, Ta 1.7, Hf 0.7, La 14.8, Ce 25.2, Pr 3.2, Sm 2.6, Eu 0.9, Tb 0.3, Gd 2.3, Dy 1.5, Ho 0.3, Er 0.8, Yb 0.7

1–10: Deformed foundation rocks; 11–14: Paradharo granodiorite. 1–5 and 10 analyzed by XRF, others wet chemically

LOI = Loss on ignition at 1000 °C. Total iron expressed as Fe_2O_3

(Middlemost 1994) to distinguish between peralkaline, alkaline and calc-alkaline rock series. Plots of the Nagar Parkar analyses on this diagram are shown in Fig. 5a. The analyses of the mafic rocks straddle the alkaline and calc-alkaline fields, whereas the rest of the analyses classify as calc-alkaline. The AFM diagram is used more commonly to distinguish between tholeiitic and calc-alkaline characteristics in sub-alkaline magma series. Dividing curves separating the rocks of the two

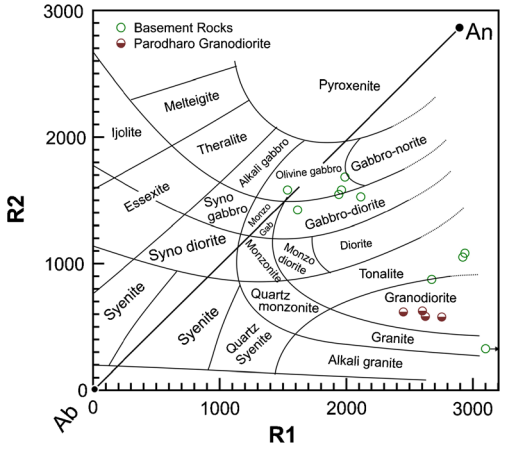

Fig. 4 Classification of the analyzed rocks, using the parameters R1 and R2, calculated from millication proportions (De la Roche et al. 1980): R1 = 4Si – 11(Na + K) – 2(Fe + Ti) and R2 = 6Ca + 2(Mg + Al)

series have been presented by several workers (Irvine and Barager 1971; Kuno 1968; Barker and Arth 1976). In Fig. 5b, all but two analyses plot in the calc-alkaline field, negating the earlier assertion (Butt et al. 1994) that the basement rocks may be tholeiitic. The two mafic rocks plotting in the tholeiite field have high amounts of opaque minerals (compare Fig. 3g), possibly as cumulate grains, or related to enrichment in Fe (and Ti) during alteration (cf. Jan and Rafiq 2007). The calc-alkaline character of the rocks is further substantiated by FeOt/MgO vs. SiO_2 relations (Miyashiro 1974). Thus, the chemistry of the rocks is in harmony with the petrographic classification of the basement rocks. The gabbro-diorite-tonalite-granodiorite-granite calc-alkaline association is commonly considered as typical of subduction-related environment.

The Shand's A/CNK vs. A/NK [where A/CNK = mole% $Al_2O_3/(CaO + Na_2O + K_2O)$, and A/NK = mole% $Al_2O_3/(Na_2O + K_2O)$] diagram has been commonly used for assessing the petrogenetic association of granitic rocks (Maniar and Piccoli 1989). Figure 6a shows the plots of the basement granitoid (tonalite, granodiorite and granite) analyses, along with the fields of analyses from various younger granitic intrusions into the basement. The field boundaries are based on the bulk data of the granitic rocks given in Ahmad and Chaudhry (2008) and 140 analyses of the four groups of the silicic rocks of Laghari (2004). The tonalite analyses classify as metaluminous whereas the Parodharo granodiorite analyses are peraluminous in character. Significantly, both sets of the analyses (barring the red granite) plot distinctly away from the Nagar Parkar A-type granitic rocks. White and Chappell (1983) used ACF diagram (A = wt% Al_2O_3 - K_2O - Na_2O, C = CaO, F = FeO(total) + MgO) for distinguishing I-type and S-type granites. On this basis (Fig. 6b), the basement tonalites plot along the boundary of the two fields, whereas the red granite and Parodharo granodiorite classify as S-Type.

Trace- and rare earth elements geochemistry

Trace elements were determined in two mafic rocks, the red granite and, along with REE, in a tonalite and a granodiorite (Table 1). A variety of diagrams based on incompatible trace elements has been devised for distinguishing within-plate, collisional, volcanic arc and oceanic-ridge granites. An island arc origin for the Nagar Parkar basement granitoids is supported by using Rb vs. Y + Nb and Nb vs Y diagrams (Pearce et al. 1984; Pearce 2015). On Rb/Zr versus Nb and Y diagrams of Brown et al. (1984), the three granitoids plot in the field of primitive island arc rocks. Whalen et al. (1987) showed that on $(Na_2O + K_2O)/CaO$ and FeO (total)/MgO vs Zn + Nb + Ce + Y diagrams A-type granites plot outside the combined field of M-, I- and S-type granites. The Nagar Parkar basement granitoids plot in the field of unfractionated M-, I- S-types. The mantle normalized multi-element spider diagram of the five basement samples is shown in Fig. 7. The overall pattern is characterized by marked spikes and troughs, and a slope from left to right, that is from LILE to HFSE. There are positive anomalies for Ba and Ce-Sr-Nd (with the exception of the

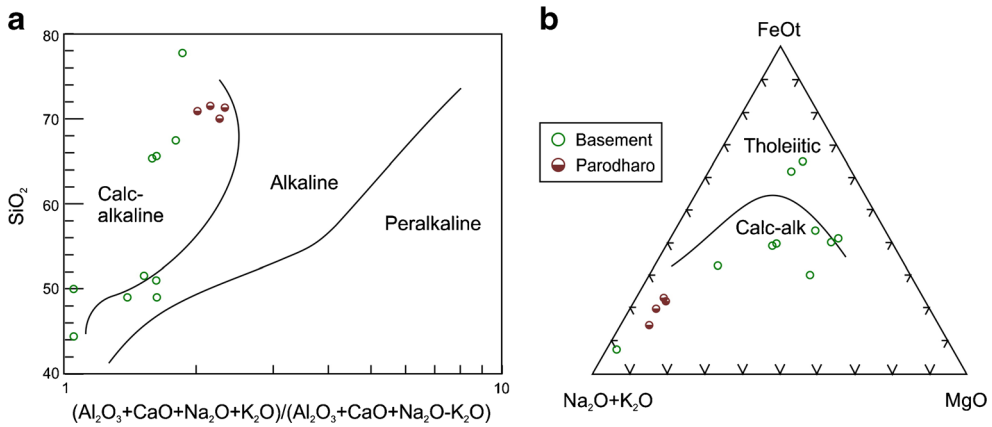

Fig. 5 Plots of the analyzed rocks on **a** SiO_2 vs $(Al_2O_3 + CaO + Na_2O + K_2O)/(Al_2O_3 + CaO + Na_2O–K_2O)$ diagram (Middlemost 1994), and **b** MgO – FeO (total) – $Na_2O + K_2O$ diagram (Irvine and Barager 1971). For more details, see text

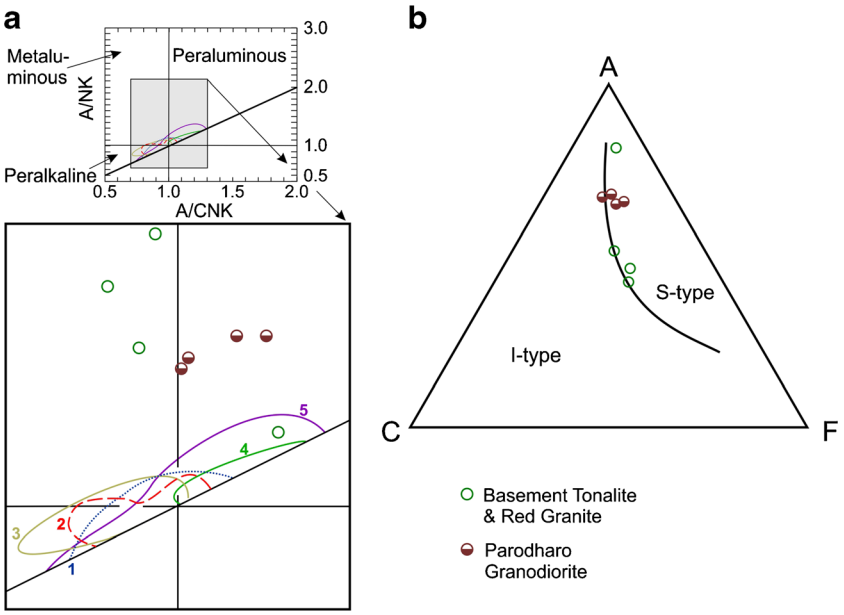

Fig. 6 **a** Classification of the basement granitoids and Parodharo granodiorite on the basis of Shand's molar indices (cf, Maniar and Piccoli 1989), A/CNK = $Al_2O_3/(CaO + Na_2O + K_2O)$ and A/NK = $Al_2O_3/(Na_2O + K_2O)$. For comparison are shown the fields of the Neoproterozoic granitic rocks from the area. 1: Gray granites, 2: Pink granites, 3: microgranites and aplites, 4: rhyolites (from Laghari 2004), and 5: various granitic rocks given in Ahmad and Chaudhry (2008). **b** A – C – K diagram (A = Al_2O_3–Na_2O–K_2O, C=CaO, F=FeO (total) + MgO) of White and Chappell (1983), showing the fields of I-type and S-type granitic rocks

red basement granite that shows negative Sr anomaly), and trough for Nb. Ti shows negative anomaly for the granitoids, but behaves oppositely in the two mafic rocks, possibly because of enrichment of opaque oxide in these, as discussed earlier. The mantle normalized incompatible trace elements, with distinct negative Nb anomaly, provide a strong support to the idea that the Nagar Parkar basement magmatism is related to subduction process. On the other hand, based on detailed geochemistry (Laghari 2004; Ahmad and Chaudhry 2008; Khan et al. 2012), within plate, A-type tectonic set up has been advocated for the Neoproterozoic granitic intrusions within the basement of the area. In the following, we substantiate the differences by comparing the geochemistry of the basement granitoids with that of the two major types of the granites that intrude them.

Notable differences can be observed between the ocean ridge granite (ORG)-normalized patterns of the two groups (Fig. 8a): (1) Average gray and pink granites are characterized by higher abundances of HFSE than the basement granitoids, (2) Ta, Ba and, especially, Sr are higher in the basement granitoids than in the granites, (3) LILE/HFSE ratio in the granites is a little lower than in the basement rocks, (4) The two groups of rocks display opposite anomalies for Ba and Ta, (5) The basement granitoids have pronounced negative Nb anomaly, and (6) Normalized patterns of basement rocks are more strongly spiked.

Comparison between the chondrite normalized REE patterns of continental granites from Skaergaard and Mull, average gray and pink granites, and the two basement granitoids is shown in Fig. 8b. All show a relative enrichment of LREE over HREE, however, the overall abundance of the REE is distinctly lower in the basement rocks than in the continental and Nagar Parkar granites. Moreover, in contrast to the basement, the granites from Skaergaard, Mull, and Nagar Parkar display a pronounced negative Eu anomaly. The lack of negative Eu anomaly and positive Ba and Sr anomalies in the basement granitoids may be related to a lack of plagioclase fractionation. In essence, then, the basement granitoids appear to be distinctly different from the later granites that intrude them. The chondrite normalized REE pattern of the Nagar Parkar gray and pink granites is quite similar to that of Mt. Abu granitoid (Ashwal et al. 2013) in Rajasthan. We noted some delicate differences in the composition of the basement granitoids and typical calc-alkaline island arc rocks, despite the compelling similarity of negative Nb anomaly. The classical island arc rocks, unlike those of the basement, have higher amounts of HREE, lower La/Nb_N, MgO, Ni and Cr, and display negative Sr anomaly. These and other chemical respects of the basement granodiorite and, to a lesser extent, tonalite are similar to adakites (Table 2). This matter is further

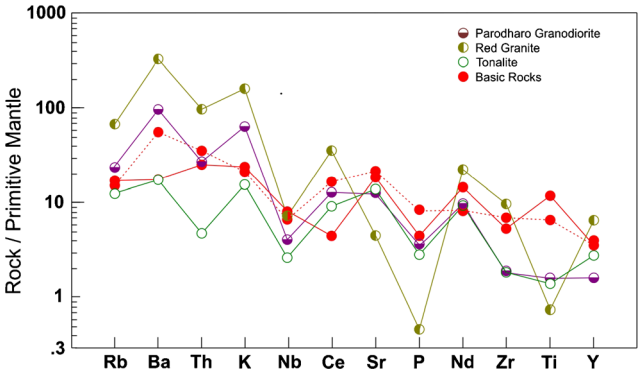

Fig. 7 Primitive mantle normalized multi element diagram of the analyzed rocks from the Nagar Parkar basement. Normalizing values are after Sun and Mcdonough 1989

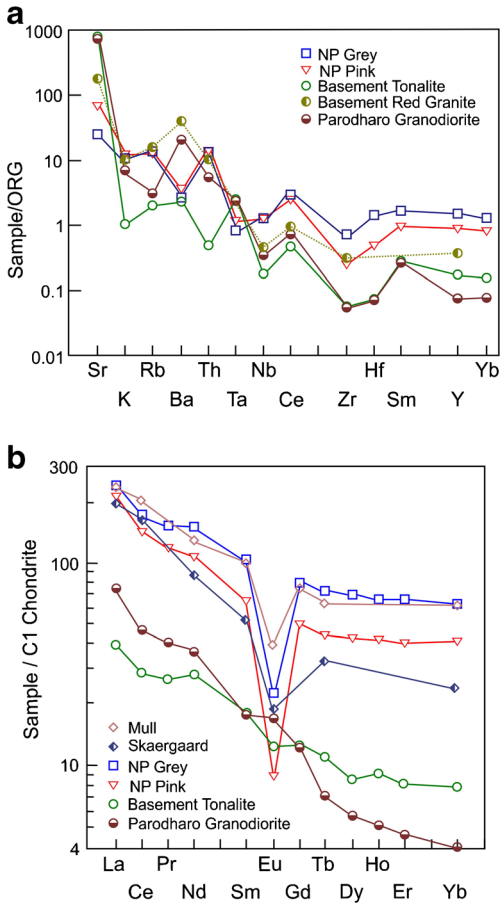

Fig. 8 **a** Ocean-ridge normalized trace element contents of the basement granitoids and Parodharo granodiorite, compared with those of the average pink and gray granites of Nagar Parkar (from Laghari 2004). Normalizing values are from Pearce et al. (1984). **b** Comparison of Chondrite normalized REE contents of the basement tonalite and Parodharo (P) granodiorite with average pink granite, average gray granite, and continental granitoids from Mull and Skaergaard. Normalizing values are after Nakamura (1974). Data for the pink and gray granites are from Laghari (2004) and those for Mull and Skaergaard from Pearce et al. (1984)

explored in the following with the help of relevant comparison with adakites and typical arc rocks.

The primitive mantle normalized trace element contents of the basement granitoids (tonalite, granite, and Parodharo granodiorite) are compared in Fig. 9a with typical Andean calc-alkaline dacite and typical adakites from Costa Rica and Equador. The Parodharo granodiorite shows a close similarity with the adakites, whereas the tonalite seems to have intermediate characteristics between the adakites and calc-alkaline dacite for the HFSES and lower normalized values for LILES. The normalized LILE-HFSE array in the tonalite, like the Andean dacite, is not as steep as in the adakites and granodiorite. Significant similarities between the granitoids and the other three subduction-related rocks include positive Ba, La, Sr and Eu anomalies and negative Nb and Ti anomalies. The red granite of the basement on this diagram, in contrast, displays negative anomalies for Sr and P, and positive anomaly for Y. Nonetheless, its overall characteristics, including negative Nb anomaly, are in line with subduction related rocks. The chondrite normalized plots of the analyses are shown in Fig. 9b, together with those of the calc-alkaline dacite, the two adakites of Fig. 9a, and typical granite from Jamaica arc. The tonalite, like the Jamaican granite, has intermediate concentrations of HREE between the dacite and adakites, but is similar to the adakite from Ecuador for the La-Gd range of elements. The Parodharo granodiorite, is similar to the adakites. As in Fig. 9a, the LREEs/HREEs ratio is higher in adakites than in typical island arc rocks ((Martin 1999). In summary, the Parodharo granodiorite appears to be adakitic, the tonalite again has an intermediate composition between adakites and typical island arc rocks.

The Adakitic traits of the basement granitoids are further explored in Fig. 10. On $(La/Yb)_N$ vs. Yb_N diagram (Fig. 10a, Hickey-Vargas et al. 1989)) and Sr/Y vs. Y diagram (Fig. 10b, Martin 1999), the Parodharo granodiorite classifies as adakite, whereas the Dhedvero tonalite

Table 2 Comparison of Nagar Parkar tonalite and granodiorite with adakites

	Adakite	Adakitic granodiorite	Basement tonalite	Parodharo granodiorite
K_2O/Na_2O	0.4–0.5	–	0.1–0.3	0.4–0.5
Mg#	0.5	–	0.5–0.6	0.4–0.5
Ni	20–40	< 4.1	21	< 5
Cr	30–50	< 8	54	6
Sr	> 300	407–532	307	295
Y	< 18	12.2–14.7	13	6.8
Yb	< 1.8	1.53–1.77	1.3	0.7
$(La/Yb)_N$	< 10–140	–	5.1	15.2
Sr/Y	> 16	31–42	23.6	43.4

Adakite data from Martin (1999)

Adakitic granodiorite, NW China, from Yin et al. (2015)

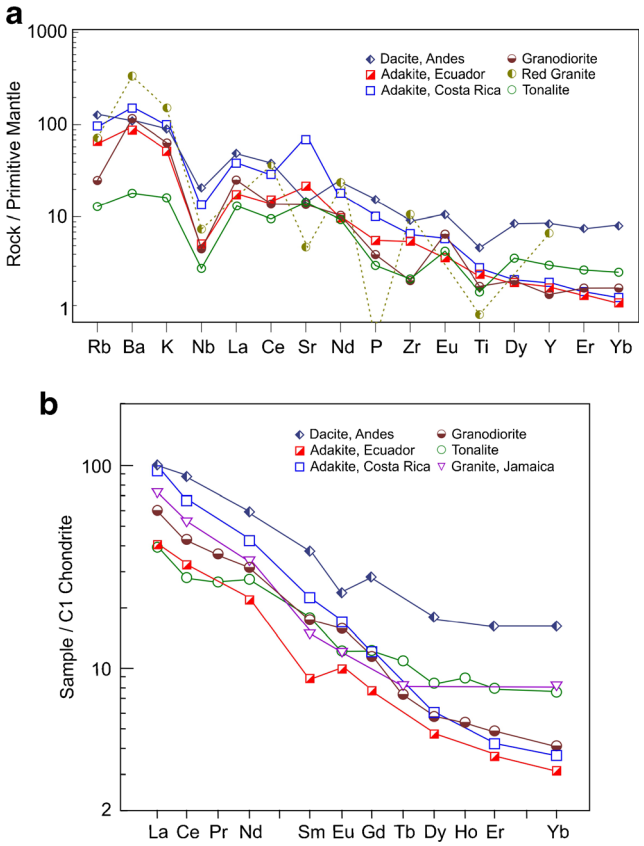

Fig. 9 Comparison of the basement granitoids (tonalite, Parodharo granodiorite and red granite) with other subduction related rocks in terms of primitive mantle normalized (**a**) and C1 Chondrite normalized (**b**) (Nakamura 1974) elemental diagrams. Typical calc-alkaline dacite from the Southern Volcanic Zone from the Andes (Hickey-Vargas et al. 1989), typical adakite from Costa Rica (Defant et al. 1992), and typical adakite from Ecuador (Samaniego 1997). Primitive mantle normalizing values are from Sun and McDonough (1989) and C1 chondrite values from Nakamura (1974)

plots in/near the overlapping area of adakites and classical island arc rocks, and the granite in the arc field. The chemical parameters for adakites (Martin 1999), together with the data for adakitic granodiorite from NW China (Yin et al. 2015), are compared with the Nagar Parkar granitoids in Table 2. There is a general similarity in the three sets of data; the tonalite has lower K_2O/Na_2O, suggesting stronger trondhjemitic characteristics than the rest. In terms of MgO vs. SiO_2 relations (Fig. 10c, Wang et al. 2006), the basement tonalite analyses plot in the field of adakites derived from subducted oceanic crust whereas those of the Parodharo granodiorite classify as thick lower crust derived adakitic rocks. This division is consistent with, respectively, the metaluminous and peraluminous classification of the two types of rocks on Shand diagram (Fig. 6a). Because of the very high SiO_2 content, the red granite plots outside the fields displayed on Fig. 10c.

Discussion and conclusions

The Nagar Parkar Igneous Complex (NPIC) is an uplifted block of mafic to felsic rocks. Earlier workers have considered it an extension of the Late Proterozoic Malani Igneous Suite (MIS) of Rajasthan. The MIS comprises three phases of magmatic rocks (Kochhar et al. 1995; Bhushan and Chandrasekaran 2002): (1) bimodal acid and basic volcanic rocks, (2) granite plutons, and (3) felsic and mafic dykes. Solanki (2011) obtained many radiometric dates on granitoids of western Rajasthan and noted that the region had passed through a complex tectono-magmatic history. It has been suggested (Dharma Rao et al. 2012) that the MIS may have developed in a subduction-related island arc environment. Ashwal et al. (2013) proposed that the Mt. Abu pluton developed in an Andean-type margin. However, most workers (Sharma 2005; Maheshwari et al. 2009; Vallinayagam and Kochhar 2011; Singh and Vallinayagam 2012) think that the MIS developed in continental extensional environment. The bimodal MIS magmatism is considered to have resulted from underplating of the continental crust by mafic magma that provided the necessary heat for extensive partial melting (Kochhar et al. 1995; Singh and Vallinayagam 2012). Such an origin is proposed for bimodal magmatism in other areas also (Winter 2010). For example, in Death Valley, California, rising basaltic magma in Cretaceous granitic basement provided heat which resulted in low-temperature thermal minimum rhyolite melts (Smith et al. 2016).

Equivalents of the first phase MIS volcanic rocks have not been reported from Nagar Parkar, but their absence can be a consequence of erosion. Our detailed studies show that the NPIC is composed of (1) mafic to granitic association of deformed rocks referred hereto as the basement, (2) undeformed granitic plutons (gray sodic alkaline granite, gray-pink and pink granite) intruding 1, and (3) abundant mafic, microgranite/aplite, rhyolite dykes intruding both 1 and 2. The basement granitoids and group 2 granites show distinct differences in petrography and geochemistry, as described above, and are magmatically not related.

The geochemical characteristics of the group 2 granites of the NPIC (high SiO_2, alkalis, Fe/Mg, Zr, Nb, Y, REE (except Eu), and low CaO, Ba and Sr) are suggestive of A-type anorogenic environment. (Laghari 2004; Ahmad and Chaudhry 2008; Khan et al. 2012). These features are shared by many of the granites and other rocks of the MIS (Bhushan and Chandrasekaran 2002; Kochhar 2008, 2009; Vallinayagam and Kochhar 2011; Singh and Vallinayagam 2012). Laghari (2004) equated the NPIC pink granite with that of Jalor, and the Karunjhar gray granite stock with the Erinpura body in Rajasthan. While there are plenty of radiometric dates on the MIS, detailed radiometric studies on the NPIC are lacking. Khan et al. (2012) reported U-Th-Pb zircon

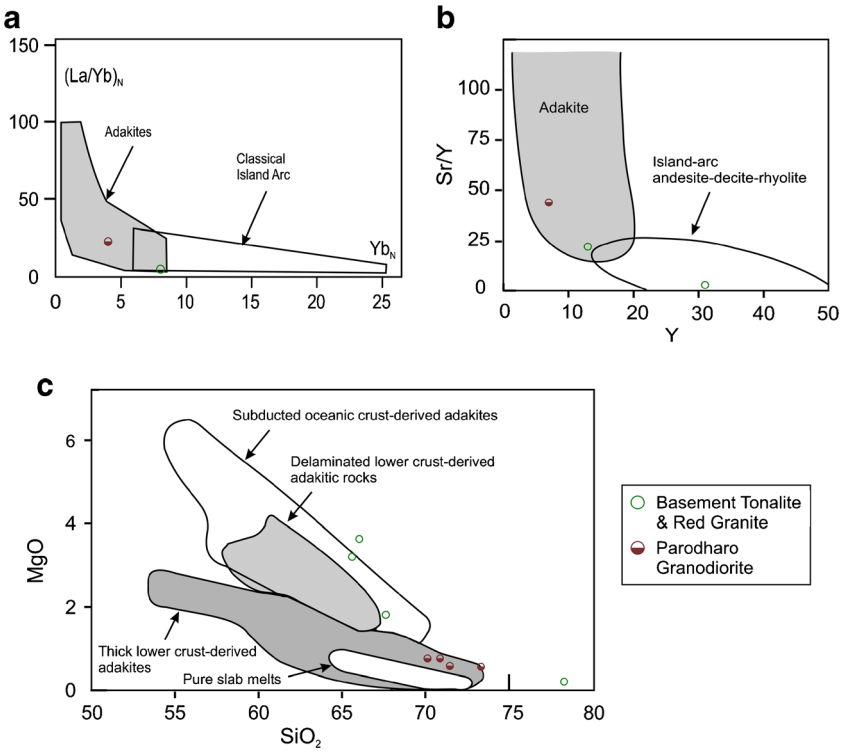

Fig. 10 Comparison of the granitoids with subduction-related rocks. In both **a** and **b** (La_N/Yb_N vs. Yb_N after Defant et al. 1992; and Sr/Y vs. Y after Martin 1999), the Parodharo granodiorite classifies as adakite, the basement tonalite plots in the overlapping area of adakites and classical island arc rocks, and the basement red granite in the classical island arc field in **b**. In terms of MgO vs. SiO_2 relations (**c**; Wang et al. 2006; cf. Yin et al. 2015l.), the tonalite analyses plot in the field of adakites derived from subducted oceanic crust whereas those of the Parodharo granodiorite classify as thick lower crust derived adakitic rocks. The granite plots outside these fields, mainly because of its very high SiO_2

ages that span from 1000 to 1100 Ma (Karunjhar gray granite) to 700–800 Ma (pink and other granites). Markhand et al. (2017) provided two U-Pb zircon ages (767 ± 12 and 803 ± 7 Ma) for the granite body of Wadhrai NW of Nagar Parkar. Unpublished U-Pb zircon ages on the Nagar Parkar granites, including the gray granite, are in conformity with the younger (< 800 Ma) ages (M. Sayab, personal communication). The zircons in porphyritic felsic dykes in the area are have similar ages (800–700 Ma) to those of the pink granites of NPIC, and are related to the main granite magmatism (Khan et al. 2017). We, therefore, reiterate that (1) The Nagar Parkar granitic plutons were emplaced in the basement after 800 Ma, and (2) Their proximity, similarity in petrography, geochemistry and radiometric dates reaffirm that they belong to the MIS. Radiometric age data are lacking on the basement. Khan et al. (2017) suggested that the granites were emplaced in 880–840 Ma old Erinpura–Nanakpur type basement rocks (e.g., Solanki 2011). A U-Pb-Th monazite age of 830 ± 0.7 Ma for the deformed red granite near Dhedvero defines the minimum age for the basement (Khan et al. 2017).

The basement rocks are mostly metaigneous, with sparse occurrence of metasedimentary rocks ranging from paragnisses and schists to quartzite. They occupy low lands between the granitic hills, probably due to their greater susceptibility to erosion and weathering. They show brittle deformation, are highly fractured and jointed, and at places also show shear foliation and plastic deformation. The igneous rocks range from mafic (abundant and possibly both plutonic and volcanic) to (quartz)diorite, tonalite, and granite, with some granodiorite, and rare hornblendite bodies. Major, trace and rare earth elements geochemistry of the rocks share the chemical characteristics, particularly low Nb content, of subduction-related rocks. Most rocks contain relics of magmatic amphibole, suggesting derivation from a hydrous magma. Water derived from dehydration of subducting slab plays a crucial role in the generation of subduction-related magmas, giving rise to amphibole-bearing rocks (Grove and Baker 1984; Iwamori 1998; Schmidt and Poli 1998; Elburg 2010). Thus, the rock association, geochemistry, and the presence of hornblende lend strong support to our proposal that the basement rocks belong to a subduction-related calc-alkaline to adakite association. Like the Erinpura pluton, which is part of the basement for MIS (Ashwal et al. 2013), they are deformed, show epidote amphibolite facie or upper greenschist facies metamorphic overprint and contain secondary epidote, amphibole, titanite, chlorite and, in mafic members, sodic plagioclase. Therefore, it is tempting to equate these rocks with the Erinpura granite, however, the trace and major element chemistry of the two is quite different. The Erinpura silicic rocks display strong negative Eu, Ba, Sr, and P anomalies (Ashwal et al. 2013). In contrast, the Nagar Parkar basement shows none of these but, instead, positive Ba and Sr anomalies (Fig. 9a).

One explanation for these differences is that the basement for the MIS is not uniform in composition.

Since the Neoproterozoic granite plutons do not show the deformation so characteristic of the basement, it is plausible that the latter was deformed before the emplacement of the granites. The Parodharo granodiorite has features typical of adakites: higher Mg#, Sr/Y and, particularly, $(La/Yb)_N$ and lower amounts of HRE and HFS elements than classical island arc granitic rocks (Martin 1986, 1999; Stewart 1992; Hastie et al. 2010). The tonalite displays intermediate geochemical characteristics between adakites and classical island arc rocks (Table 2), whereas the red granite is akin to the latter. In a series of diagrams (Figs. 8 and 9), the trace and RE element contents of the granitoid members of the basement are compared with those of the younger Neoproterozoic granites of Nagar Parkar, within-plate granites from Mull and Skaergaard, island arc granite from Jamaica, typical calc-alkaline dacite from the Andes, and typical adakites from Costa Rica and Ecuador. Important conclusions can be readily drawn from this comparison, such as, (1) Nagar Parkar basement granitoids are different from the two major varieties (pink and gray) of the Neoproterozoic granite which intrude them, (2) The latter are similar to the continental granites of Mull and Skaergaard, (3) The granodiorite is closer to typical adakites than to typical calc-alkaline dacite from the Andes, and (4) The tonalite has intermediate chemistry between classical island arc rocks and typical adakites.

In summary, the subduction-related nature of the basement supports the idea that these rocks may have formed in a continental margin or island arc setting. Closure of the intervening ocean and suturing with a landmass may have caused the pervasive deformation and low-grade metamorphism. Subsequently, when the arc had become a part of the Gondwana, A-type granites were emplaced. The geochemistry of the basement granodiorite, and to a lesser extent tonalite, especially their rather high Sr/Y and La/Yb ratios, suggest that they have adakitic affinities. The red granite, on the other hand, is compositionally akin to classical island arc rocks. Negative Nb anomaly and MgO-SiO_2 relations support that the tonalities may be derived from subducted oceanic crust or upper mantle, while the granodiorite may be derived from thickened lower crust. Their steep normalized REE pattern is suggestive of garnet and/or amphibole residue, and lack of negative Eu anomaly coupled with positive Sr anomaly suggest lack of plagioclase fractionation. A number of tectonic models have been proposed for the MIS and its equivalents in Seychelles, Madagascar and elsewhere in "Rodinia." On basis of limited data, we would not like to engage in this exercise, but the basement may be representing an island arc or Andean-type continental margin that developed prior to suturing and amalgamation in the Gondwana, and intrusion of A-type granites. The magmatic arc may be related to the eastward subduction and closure of the Mozambique ocean.

Acknowledgements We thank our parent organizations for the use of facilities and logistic support. The research was partially funded by a grant of the Pakistan Academy of Sciences to M.Q. Jan. M. Tahir Shah is thanked for advice during the major element analysis, Suhail Anjum for his support during the field work, and Ikram Abbasi for drafting of figures. Last, but not least, we are thankful to Professor AM Al-Amri, and two anonymous reviewers for useful suggestions for improvement of the manuscript.

References

Ahmad SA, Chaudhry MN (2008) A-type granites from the Nagar Parkar complex, Pakistan: geochemistry and origin. Geol Bull Punjab Uni 43:69–81

Ashwal LD, Solanki AM, Pandit MK, Corfu F, Hendriks BWH, Burke K, Torsvik TH (2013) Geochronology and geochemistry of Neoproterozoic Mt. Abu granitoids, NW India: regional correlation and implications for Rodinia paleogeography. Precambrian Res 236: 265–286. https://doi.org/10.1016/j.precamres.2013.07.018

Barker F, Arth JG (1976) Generation of trondhjemitic-tonalitic liquids and Archean bimodal trondhemite-basalt suites. Geology 4(10): 596–600

Bhushan SK, Chandrasekaran V (2002) Geology and geochemistry of the magmatic rocks of the Malani igneous suite and tertiary alkaline province of western Rajasthan. Geol Surv India Memoir 126, 114 pp

Brown GC, Thorpe RS, Webb PC (1984) The geochemical characteristics of granitoids arcs and comments on magma sources. J Geol Soc Lond 141(3):413–426. https://doi.org/10.1144/gsjgs.141.3.0413

Butt KA, Nazirullah R, Syed SH (1989) Geology and gravity interpretation of Nagar Parkar area and its potential for surficial uranium deposits. Kashmir J Geol 6 & 7:41–50

Butt A., Jan MQ, Karim A (1994) Late Proterozoic rocks of Nagar Parkar, southeastern Pakistan: a preliminary petrologic account. In: Geology in South Asia-1, Ahmed R, Sheikh AM (eds) Hydrocarbon Development Institute of Pakistan, Islamabad, pp 106–109

Davidson J, Turner S, Handley H, Macpherson C, Dosseto A (2007) Amphibole sponge in arc crust. Geology 35(9):787–790. https://doi.org/10.1130/G23637A.1

De la Roche H, Leterrier J, Grandle Claude P, Marchal M (1980) A classification of volcanic and plutonic rocks using R1–R2 diagrams and major element analyses- its relationships and current nomenclature. Chem Geol 29:193–210

Debon F, Le Fort P (1988) A cationic classification of common plutonic rocks and their magmatic associations: principals, method, application. Bull Mineral 111:493–510

Defant MJ, Jackson TE, Drummond MS, De Boer JZ, Bellon H, Feigenson MD, Maury RC, Stewart RH (1992) The geochemistry of young volcanism throughout western Panama and southeastern Costa Rica: an overview. J Geol Soc Lond 149(4):569–579. https://doi.org/10.1144/gsjgs.149.4.0569

Dharma Rao CV, Santosh M, Kim SW (2012) Cryogenian volcanic arc in the NW Indian shield: zircon shrimp U-Pb geochronology of felsic tuffs and implications for Gondwana assembly. Gondwana Res 22: 36–53

Elburg MA (2010) Sources and processes in arc magmatism: the crucial role of water. Geol Belg 13:121–136

Grove TL, Baker MB (1984) Phase equilibrium controls on the tholeiitic versus calc-alkaline differentiation trends. J Geophys Res 89(B5): 3253–3274. https://doi.org/10.1029/JB089iB05p03253

Hastie AR, Kerr AC, McDonald I, Mitchell SF, Pearce JA, Millar IL, Barfod D, Mark DA (2010) Geochronology, geochemistry and petrogenesis of rhyodacite lavas in eastern Jamaica: a new adakite subgroup analogous to early Archaean continental crust? Chem Geol 276(3-4):344–359. https://doi.org/10.1016/j.chemgeo.2010.07.002

Hickey-Vargas R, Moreno Rao H, Lopez Escobar L, Frey FA (1989) Geochemical variations in Andean basaltic and silicic lavas from the Villerica-Lenin volcanic chain (39.5o S): an evaluation of source heterogeneity, fractional crystallization and crustal contamination. Contrib Mineral Petrol 103(3):361–386. https://doi.org/10.1007/BF00402922

Irvine TN, Barager WRA (1971) A guide to the chemical classification of the common volcanic rocks. Can J Earth Sci 8:523–548

Iwamori H (1998) Transportation of H2O and melting in subducting zones. Earth Planet Sci L ett 160(1-2):65–80. https://doi.org/10.1016/S0012-821X(98)00080-6

Jan MQ, Rafiq M (2007) Petrology of chloritoid-ilmenite-rich rocks in the Indus suture melange of Pakistan: implications for the cretaceous paleolatitude of Kohistan. J Asian Earth Sci 29(2-3):361–368. https://doi.org/10.1016/j.jseaes.2006.07.010

Jan MQ, Laghari A, Khan MA (1997) Petrography of the Nagar Parkar igneous complex. Tharparkar, southeastern Sindh, Pakistan. Geol Bull Univ Peshawar 30:227–259

Jan MQ, Agheem MH, Laghari A, Anjum S (2014) Geology and petrography of the Nagar Parkar igneous complex, southeastern Sindh: the Dinsi body. J Himal Earth Sci 47:1–14

Jan MQ, Agheem MH, Laghari A, Anjum S (2016) Geology and petrography of the Nagar Parkar igneous complex, southeastern Sindh: the Wadhrai body. J Himal Earth Sci 49(1):17–29

Jan MQ, Agheem MH, Laghari A, Anjum S (2017) Geology and petrography of the Nagar Parkar igneous complex, southeastern Sindh, Pakistan: the Kharsar body. J Geol Soc India 89(1):91–98. https://doi.org/10.1007/s12594-017-0564-4

Kazmi AH, Jan MQ (1997) Geology and tectonics of Pakistan. Graphic Publishers, Karachi

Kazmi AH, Khan RA (1973) Report on the geology, minerals and water resources of Nagar Parkar, Pakistan. Geol Surv Pak, Info Release 64

Khan T, Murata M, Rehman HU, Zafar M, Ozawa H (2012) Nagar Parker granites showing Rodinia remnants in the southeastern part of Pakistan. J Asian Earth Sci 59:39–51. https://doi.org/10.1016/j.jseaes.2012.05.028

Khan T, Murata M, Jan MQ, Rehman HU, Zafar M, Ozawa H, Qadir A, Mehmood S (2017) Felsic dykes in the Neoproterozoic Nagar Parkar igneous complex, SE Sindh, Pakistan: geochemistry and tectonic settings. Arab J Geosci 10(14):308. https://doi.org/10.1007/s12517-017-3077-y

Kochhar N (2008) A-type Malani magmatism: signatures of the Pan-African event in the northwest Indian Shield assembly of the Late Proterozoic Malani supercontinent. Geol Surv India Spec Pub 91:112–126

Kochhar N (2009) The Malani supercontinent: Middle East connection during Late Proterozoic. In: Shrivastava KL (ed) Economic mineralization. Scientific Publishers, Jaipur, pp 15–25

Kochhar N, Dhar S, Sharma R (1995) Geochemistry and tectonic significance of acid and basic dykes associated with Jalor magmatism, west Rajasthan. Geol Soc India Mem 33:375–389

Kuno H (1968) Differentiation of basalt magmas. In: Basalt; the Poldervaart treatise on rocks of basaltic composition. Wiley, New York, 2:623–688

Laghari A (2004) Petrology of the Nagar Parkar granites and associated basic rocks, Thar District, Sindh, Pakistan. PhD thesis, Uni Peshawar

Maheshwari A, Coltorti M, Rajput SK, Verma M (2009) Geochemical characteristics, discrimination and petrogenesis of Neoproterozoic peralkaline granites, Barmer district, SW Rajasthan, India. Int Geol Rev 51(12):1103–1120. https://doi.org/10.1080/00206810902895337

Maniar PD, Piccoli PM (1989) Tectonic discrimination of granitoids. Geol Soc Am Bull 101(5):635–643

Markhand AH, Xia Q, Agheem MH, Jia L (2017) U-Pb zircon dating and geochemistry of the rocks at Wadhrai body, Nagar Parkar igneous complex, Sindh, Pakistan. Sindh Univ Res J (Sci Ser) 49(1):01–06

Martin H (1986) Effect of steeper Archaean geothermal gradients on geochemistry of subduction-zones magmas. Geology 14(9):753–756

Martin H (1999) Adakitic magmas: modern analogues of Archaean granitoids. Lithos 46(3):411–426. https://doi.org/10.1016/S0024-4937(98)00076-0

Middlemost EAK (1994) Naming materials in the magma igneous rock system. Earth Sci Rev 37(3-4):215–224. https://doi.org/10.1016/0012-8252(94)90029-9

Miyashiro A (1974) Volcanic rock series in island arcs and active continental margins. Am J Sci 274(4):321–355. https://doi.org/10.2475/ajs.274.4.321

Muslim M, Akhtar T, Khan ZM, Khan T (1997) Geology of the Nagar Parkar area, Tharparkar district, Sindh, Pakistan. Geol Surv Pak, Info Release 605

Nakamura N (1974) Determination of REE, Ba, Fe, Mg, Na and K in carbonaceous and ordinary chondrites. Geochim Cosmochim Acta 38(5):757–775. https://doi.org/10.1016/0016-7037(74)90149-5

Pearce J (2015) Trace elements in granites: indicators of tectonic settings and mineralization potential. In: Second International Workshop on Tethyan orogenesis and Metallogeny in Asia, October 16—21, 2015, Wuhan, China, pp 112–115

Pearce JA, Harris NBW, Tindle AG (1984) Trace element discrimination diagrams for the tectonic interpretation of granitic rocks. J Petrol 25(4):956–983. https://doi.org/10.1093/petrology/25.4.956

Samaniego P (1997) Interrelations entre les magmas adakatiques et calco-alcalins: geochemie des complexes volcaniques du Moranda-Fuya (Equateur). Mem, Uni Clermont-Ferrund

Schmidt MW, Poli S (1998) Experimentally-based water budget for dehydrating slabs and consequences for the magma generation. Earth Planet Sci Lett 163(1-4):361–379. https://doi.org/10.1016/S0012-821X(98)00142-3

Sharma KK (2005) Malani magmatism, an extensional lithospheric tectonic origin. Geol Soc Am Spec Pap 388:463–476

Singh LG, Vallinayagam G (2012) Petrological and geochemical constraints in the origin and mineralization of A-type granite suite of the Dhiran area, northwestern peninsular India. Geoscience 2:66–80

Smith DJ (2014) Clinopyroxene precursors to amphibole sponge in the crust. Nat Commun 5. https://doi.org/10.1038/ncomms5329

Smith EI, Tibbetts A, Belmontes H, Johnsen R, Walker JD (2016) Pliocene basaltic and rhyolitic volcanism in the Greenwater range, Death Valley area, California. In: Proceedings, natural history conference, Death Valley natural history association, 3–43. https://www.researchgate.net/publication/285234149

Solanki AM (2011) A petrographic, geochemical and geochronological investigation of deformed granitoids from SW Rajasthan: Neoproterozoic age of formation and evidence of Pan-African imprint. MSc thesis, Uni Witwatersrand

Stewart RH (1992) The geochemistry of young volcanism throughout western Panama and southeastern Costa Rica: an overview. J Geol Soc Lond 149:569–579

Sun SS, Mcdonough WF (1989) Chemical and isotopic systematics of ocean basalts: implication for mantle composition and processes. In: Saunders AD, Norry MJ (eds) Magnetism in the ocean basins, vol. 42. Geol Soc, London, Spec Pub 42:313–345

Vallinayagam G, Kochhar N (2011) Petrological evolution and emplacement of Siwana and Jalor ring complexes of Malani Igneous Suite, northwestern peninsula India. In: Ray J, Sen G, Ghosh B (eds)

Topics in igneous petrology. Springer, pp 437–448. https://doi.org/10.1007/978-90-481-9600-5_17

Wang Q, JF X, Jian P, Bao ZW, Zhao ZH, Li CP, Xiang KL, Ma JL (2006) Adakitic porphyries in an extensional tectonic setting, Dexing, South China: implications for the genesis of porphyry copper mineralization. J Petrol 47(1):119–144. https://doi.org/10.1093/petrology/egi070

Whalen J, Currie KL, Chappell BW (1987) A-type granites: geochemical characteristics, discrimination and petrogenesis. Contrib Miner Petrol 95(4):407–419. https://doi.org/10.1007/BF00402202

White AJR, Chappell BW (1983) Granitoid types and their distribution in the Lachlan fold belt, southeastern Australia. In: Roddick JA (ed) Circum-Pacific Plutonic Terranes. Geol Soc Am Mem 159:21–34

Winter JD (2010) Principals of igneous and metamorphic petrology. Pearson Education Inc, New Jersey

Yin J, Chen W, Xiao W, Yuan C, Windley BF, Yu S, Cai K (2015) Late Silurian-early Devonian adakitic granodiorite, A-type and I-type granites in NW Junggar, NW China: Partial melting of mafic lower crust and implications for slab roll-back. Gondwana Res. https://doi.org/10.1016/j.gr.2015-06-016